"Plug-n-Play" Sensing with Digital Microfluidics

Richard P. S. de Campos,[†,‡,⊥] Darius G. Rackus,[†,‡,⊥] Roger Shih,[†,‡] Chen Zhao,[§] Xinyu Liu,[§] and Aaron R. Wheeler*[,†,‡,∥]

[†]Department of Chemistry, University of Toronto, 80 St. George Street, Toronto, Ontario M5S 3H6, Canada

[‡]Donnelly Centre for Cellular and Biomolecular Research, 160 College Street, Toronto, Ontario M5S 3E1, Canada

[§]Department of Mechanical and Industrial Engineering, University of Toronto, 5 King's College Road, Toronto, Ontario M5S 3G8, Canada

[∥]Institute of Biomaterials and Biomedical Engineering, University of Toronto, 164 College Street, Toronto, Ontario M5S 3G9, Canada

S Supporting Information

ABSTRACT: Digital microfluidics (DMF) is a platform that enables highly reconfigurable and automated fluidic operations using a generic device architecture. A unique hallmark of DMF is its "flexibility": a generic device design can be used and reused for many different, divergent fluidic operations. The flexibility of DMF is compromised when devices are permanently modified with embedded sensors. Here we introduce a solution to the "flexibility gap" between fluidic operations in digital microfluidics and embedded sensors: "plug-n-play DMF" (PnP-DMF). In PnP-DMF, devices are designed to allow for rapid and seamless exchange of sensors depending on the application needs. This paper provides "proof of concept" for PnP-DMF using commercial biosensors for glucose and β-ketone, a custom paper-based electrochemical sensor for lactate, and a generic screen-printed electroanalytical cell. We demonstrate that hot-swapping sensors between experiments allows for convenient implementation of complex processes such as automated analysis of blood samples by standard addition. Finally, we explored the suitability for using PnP sensors in tandem with other sensing modalities, combining biosensor-based electrochemical measurement of glucose with a chemiluminescent magnetic bead-based sandwich immunoassay for insulin. The latter is notable, as it constitutes the first report of an analysis of different analytes in both the supernatant and precipitate from a single sample-aliquot in a microfluidic device. The results presented here highlight the versatility of PnP-DMF, illustrating how it may be useful for a wide range of applications in diagnostics and beyond.
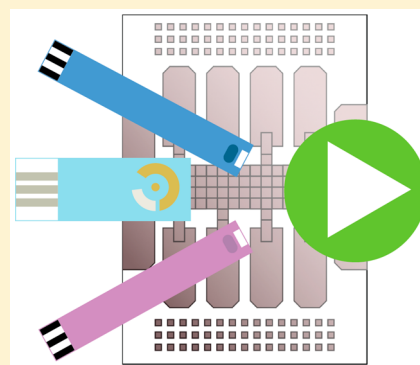
M ost microfluidic diagnostic devices described previously are based on enclosed microchannels,[1] but other formats such as paper microfluidics[2] and digital microfluidics (DMF) have also been used.[3] Of these various microfluidic formats, DMF is particularly well suited to recapitulate laboratory operations in a manner that preserves the flexibility inherent to lab-work.[4] In DMF, discrete droplets of liquids are manipulated on an array of insulated electrodes. In the most common "two-plate" DMF format, the droplets are sandwiched between a hydrophobic-coated top-plate (DMF ground electrode) and a hydrophobic bottom plate bearing an array of "driving" electrodes coated by a dielectric insulator. In this paradigm, droplets can be dispensed, split, mixed, and merged[5] to perform a variety of automated routines and assays. Because devices comprise a generic array of electrodes, droplet actions can be reconfigured (as opposed to alternate formats where fluid options are "programmed" into the arrangement of channels that are permanently built-in to the device) and virtually any desired combination of operations can be performed with a single device architecture. Recently, a demonstration of portable DMF diagnostics was reported,[3]

highlighting the utility of this platform for in-the-field applications.

The flexibility of DMF is perfectly matched by optical detectors that can be moved and changed depending on the application. However, optical sensors often require bulky controllers, light sources, and optical components, which are not ideal for portable applications in the field. In contrast, DMF devices bearing embedded sensors relying on electrochemistry[6−10] or other transducers[11−16] can be well suited for building small-form-factor instruments for field applications. (As a non-DMF example, the Abbott i-STAT, which relies on microchannels integrated with miniaturized electroanalytical sensors, is arguably the world's most successful portable diagnostic instrument.[17]) Unfortunately, the inherent flexibility of DMF is compromised when devices are permanently modified with embedded components. That is, the act of permanently integrating a biosensor into a DMF

device (e.g., an electroanalytical cell in which the working electrode is functionalized with an enzyme and electron mediators) dedicates it for use with only a single assay or procedure, greatly narrowing the scope of what it can do.

Here we introduce a solution to the "flexibility gap" between fluidic operations in digital microfluidics and embedded sensors: "plug-n-play DMF" (PnP-DMF). In PnP-DMF, the top-plates of DMF devices are designed to seamlessly couple with prefabricated sensors. The sensor-exchange process is rapid, leading to what we call "hot swapping" or exchanging sensors between experiments on a given device. We demonstrated "proof of concept" for PnP-DMF by application to serial and parallel measurements of mixtures of glucose, β-ketone, and lactic acid. To explore applicability beyond commercial biosensors, we also evaluated the integration of custom paper-based electrochemical lactate sensors and generic screen-printed electrode cells. Finally, we explored the suitability for using PnP sensors in tandem with other sensing modalities, combining biosensor-based electrochemical measurement of glucose with a chemiluminescent magnetic bead-based sandwich immunoassay for insulin. We refer to this parallel use of two different detectors as "multimodal" detection and note that this is the first report of this type of scheme in digital microfluidics. This is also is the first report, to our knowledge, of analysis of different analytes in both the supernatant and precipitate from a single sample-aliquot in any type of microfluidic device. The results presented here highlight the versatility of PnP-DMF, illustrating how it may be useful for a wide range of applications in the laboratory and the field.

■ METHODS

If not stated otherwise, all reagents were purchased from Sigma-Aldrich. Unless indicated otherwise, all solutions used on DMF were supplemented with 0.1% (w/v) Tetronic 90R4 (BASF Corp.).

DMF Device Fabrication and Assembly. DMF bottom plates were fabricated from Cr-coated glass substrates (Telic Co.) at the University of Toronto Nanofabrication Centre (TNFC) using methods reported previously.[18] For most experiments, bottom plates included an array of DMF driving electrodes denoted "design 1": a 15 × 4 array of square driving electrodes (2.2 mm × 2.2 mm each), 12 large reservoir electrodes (16.4 mm × 6.7 mm), and 8 dispensing electrodes (2.2 mm × 4.4 mm). For other experiments, "design 2" was used: 92 roughly square interdigitated electrodes (2.8 mm × 2.8 mm), 10 reservoir electrodes (10 mm × 6.7 mm), and 10 dispensing electrodes (5.2 mm × 2.4 mm). After forming the DMF driving electrodes, device bottom-plates were coated with a layer of Parylene C in a dedicated chemical vapor deposition instrument (Specialty Coating Systems,) (~7 μm thick) and a layer of Teflon-AF (Chemours) by spin-coating at 2000 rpm followed by baking at 160 °C for 15 min (~70 nm thick).

Custom DMF top plates were fabricated from indium tin oxide (ITO)-coated polyethylene terephthalate (PET) films (60 Ω/sq surface resistivity, Sigma). The method is illustrated in Supplementary Figure S1. Briefly, a 40 W H-series desktop CO$_2$ laser (Full Spectrum Laser) was used to cut the ITO-PET film into 75 mm × 25 mm pieces and to cut one or more triangular apertures (equilateral with 1.5 mm sides) through each piece. The conductive side of the substrates were then coated with 1% (w/v) FluoroPel PFC 1101 V (Cytonix LLC)

by spin-coating at 2000 rpm for 30 s followed by baking at 110 °C for 15 min. PMMA sheets (1.5 mm thick, Plastic World) were laser-cut into 75 mm × 24 mm backing pieces, each with one or more 15 mm × 6 mm or 27 mm × 11 mm rectangular cutouts (with the long-axis of each cutout parallel to the long-axis of the substrate) formed at one of the 24 mm-wide edges. Each top plate was assembled by adhering the nonconductive, non-Fluoropel-coated side of an ITO-PET substrate to a PMMA backing via pressure sensitive silicone adhesive (Adhesives Research), aligned such that each triangular aperture in the ITO-PET layer lined up with an end of a rectangular cut-out in the PMMA backing. DMF devices were then assembled by joining a top plate to a bottom plate via two pieces of double-sided tape (3M Company, Maplewood, MN). This arrangement forms an interplate spacing of ~180 μm, defining the volume of a single-unit droplet (i.e., a droplet dispensed over a single electrode) to approximately 800 nL or 1 μL on DMF devices formed withdesigns 1 and 2, respectively.

Sensor Integration. Four types of sensors were integrated with DMF top-plates, including two commercial biosensors, a custom paper-based biosensor, and a commercial screen-printed electrode cell. The two commercial biosensors are outlined in detail in Supplementary Figure S2 and were specific for glucose and β-ketone (ART08009 Rev. B 1/06 and ART07249 Rev. C 1/06, Abbott Diabetes Care). The custom paper-based biosensor for lactate is outlined in detail in Supplementary Figure S3 and was formed using methods similar to those described previously.[19] Briefly, paper substrates (35 mm × 8.5 mm, Whatman 1 Chr) were modified to include three screen-printed carbon electrodes (E3456, Ercon) positioned over a patterned circular test zone (4 mm radius) with hydrophobic boundaries defined by wax printing (ColorQube 9570, Xerox). The side of the substrate opposite from the electrodes was kept hydrophilic to allow sample flow through the paper. Before use, each paper-based sensor was treated by incubating with 3 μL of electron mediator solution (200 mM K$_3$[Fe(CN)$_6$] in 1 M KCl) and then 3 μL of 200 U/mL lactate oxidase, with each incubation step followed by an air-drying step (~5 min). Each carbon electrode was connected to a silver ink (E1660, Ercon) trace to allow for electrical connections. Finally, the screen-printed electrode cells (DRP-C223AT, DropSens) are outlined in detail in Supplementary Figure S4.

At the beginning of each experiment (and in any "hot swap" in an ongoing experiment), a sensor was mated with a DMF device in 2−4 stages. In the first stage (when relevant), the sensor and wick that had been used previously were removed. In the second stage, a ~1 mm × 1 mm KimWipe tissue wick (Kimberly-Clark) was inserted into the triangular aperture in the ITO-PET substrate. In the third stage, the sensor was inserted into the appropriate cut-out in the PMMA backing (15 mm × 6 mm for commercial biosensors, 19 mm × 9 mm for paper biosensors, or 27 mm × 11 mm for screen-printed electrodes). For the screen-printed electrodes, a fourth stage was added; an additional 10 mm × 10 mm Whatman No. 1 filter paper substrate was placed between the aperture and the screen-printed electrodes to allow fluidic contact between the sample and the electrodes. In experiments using both commercial biosensors and paper biosensors for serial reading, a top plate with the larger cut-out (19 mm × 9 mm) was used, and the glucose and β-ketone biosensors were aligned with the

help of a removable PMMA inset piece that adjusted the size down to the smaller size (15 mm × 6 mm).

A custom manifold was built to make electrical connections to the commercial biosensors. The manifold comprised a 3D printed (MakerBot 2.0) polylactic acid housing and a copper circuit-board milled using a computer numerical control machine (Othermill V2, Other Machine Co.). The circuit board comprised three copper contacts with the same pitch as the biosensor electrodes. Copper traces lead to header pins (Digi-Key) where connections to the potentiostat were made.

Device Operation. Digital microfluidic devices were interfaced via pogo-pin connectors to the open-source DropBot control system (http://microfluidics.utoronto.ca/dropbot/) and droplet movement (driven by applying voltages of 85−110 V_{RMS} at 10 kHz) was programmed by MicroDrop software as described previously.[20] Dispensing was performed by loading a solution into a reservoir (6−10 μL), activating a series of electrodes extending from the reservoir, and deactivating the rectangular dispensing electrode, thus pinching off a single-unit droplet (0.8 or 1.0 μL depending on the design). Merging two single-unit droplets formed a double-unit droplet (1.6 or 2.0 μL), merging a double-unit droplet with a third single-unit droplet formed a triple-unit droplet (2.4 or 3.0 μL), and so on. Mixing was achieved by moving a merged droplet over a series of eight electrodes in a circular pattern for 30 s. Splitting of double-unit droplets into single-unit droplets was achieved by activating a linear series of three electrodes and then turning off the middle electrode for 5 s, resulting in two single-unit droplets. A similar procedure was implemented for splitting quadruple-unit droplets into double-unit droplets, in which a linear series of five electrodes were activated and then the middle electrode was turned off for 5 s. In some experiments, to estimate droplet volumes, droplets on DMF devices were photographed with a USB microscope (Adafruit). The droplet area was measured using ImageJ and multiplied by a gap height of 180 μm to calculate the droplet volume.

Electrochemical Measurements. An open-source DStat potentiostat[21] (http://microfluidics.utoronto.ca/dstat) was used to program and perform all electrochemical measurements. The DStat control software was connected to the MicroDrop DMF control software by means of a plugin. Commercial biosensors (Figure S2) were operated in a three-electrode configuration, with the carbon electrode used as the working electrode (WE), the large U-shaped Ag/AgCl electrode used as the counter electrode (CE), and the small Ag/AgCl electrode used as the reference electrode (RE). Amperometric measurements were collected at the manufacturer-recommended setting (+0.200 V vs Ag/AgCl) for 30 s; the signal measured at 5 s was recorded for quantitation. For off-chip measurements, 2 μL of glucose or β-hydroxybutyrate solutions in PBS with 4% (w/v) bovine serum albumin (BSA) in PBS were pipetted directly onto the active area of a biosensor and then analyzed. Custom paper-based biosensors (Figure S3) were operated in the three-electrode mode, with screen-printed carbon electrodes used as WE, CE, and pseudo-RE electrodes. Amperometric measurements were collected at +0.450 V vs carbon pseudo-RE for 30 s, and the signal measured at 5 s was recorded. Commercial screen-printed electrode cells (Figure S4) were operated in a three-electrode configuration with Au WE and CE and a Ag pseudo-RE. Amperometric measurements were collected at +0.800 V vs Ag for 10 s; the signal measured at 5 s was recorded for

quantitation. Calibration curves were formed by plotting current measurements (collected on- or off-chip) relative to concentration, and a line of best fit was determined using least-squares analysis in GraphPad Prism 6. The limit of detection (LOD) and limit of quantitation (LOQ) were defined as the concentrations corresponding to the mean signal of the blank plus 3 or 10 standard deviations of the blank, respectively.

PnP-DMF Single-Mode Electrochemical Measurements. The new system was used for three single-mode applications (I−III), all in devices generated with design 1 (see above). In the first application (I), two sets of multiplexed electrochemical measurements were performed to evaluate performance in serial and in parallel modes. In the first set of experiments (Ia), the test solution comprised 5 mM glucose, 5 mM β-hydroxybutyrate, and 4% (w/v) BSA in PBS. For serial measurements, a DMF device was assembled with a glucose biosensor in a single cut-out in a top plate. Test solution was pipetted onto a device reservoir, and a double-unit droplet was dispensed and delivered to the biosensor. After measurement, the biosensor and absorbent wick were removed. A fresh wick was inserted into the aperture and a β-ketone biosensor was installed. A second double-unit droplet of the test solution was dispensed and delivered to the β-ketone biosensor for measurement. For parallel measurements, a top plate with two cutouts was used, such that a glucose and a β-ketone biosensor could both be installed. Test solution was pipetted onto a device reservoir, and two double-unit droplets were dispensed on to the array and delivered to the test strips. The potentiostat was first connected to the glucose biosensor and then connected to the β-ketone biosensor to make the two measurements.

In the second set of experiments (Ib) in the first single-mode application, serial analysis was applied to evaluate test solutions containing different combination of analytes, including 5 mM glucose (+Glu), and/or 12.5 mM lactate (+Lac), and/or 5 mM β-hydroxybutyrate (+Ket) in PBS. In typical experiments, one of the test solutions [either (+Glu, −Lac, + Ket), (+Glu, +Lac, −Ket), (−Glu, +Lac, +Ket) or (+Glu, +Lac, +Ket)] was loaded into a device with a glucose biosensor. A double-unit droplet was dispensed and delivered to the sensor, and after measurement, the sensor and wick were removed. A β-ketone biosensor and wick were then installed, and a second double-unit droplet was dispensed and delivered to the sensor. After measurement, the sensor and wick were removed. Finally, a paper-based lactate biosensor and wick were installed, and the remaining sample volume on the chip ($\sim$6.0 μL) was delivered to the sensor and measured. This procedure was repeated for all test-solutions.

In the second single-mode application (II), the glucose concentration in blood was measured by electrochemistry on DMF devices by standard additions in two stages. In the first stage, a four-droplet dilution series of glucose was formed on-chip [in diluent, PBS with 4% (w/v) BSA]. Briefly, aliquots of diluent and 12 mM glucose (in diluent) were pipetted into separate reservoirs on a device. One single-unit droplet of 12 mM glucose was dispensed and stored on the array. A second single-unit droplet of 12 mM glucose was dispensed, as was a single-unit droplet of diluent, and the two were merged and mixed. The resulting double-unit droplet of 6 mM glucose was split into two single-unit droplets; one split-droplet was stored on-chip, the other split-droplet was merged and mixed with a single-unit droplet of diluent. The resulting double-unit droplet of 3 mM glucose was split into two single-unit droplets; one

split-droplet was stored and the other was removed to waste. Last, a fourth single-unit droplet of diluent was dispensed and stored. In the second stage, the dilution series (i.e., the four single-unit droplets formed as described above) was mixed with human whole blood (ZenBio) and analyzed. Briefly, whole blood was pipetted into a reservoir, and four double-unit droplets were dispensed onto the array. Each of the double-unit droplets of blood was merged and mixed with one of the single-unit droplets containing 0 mM, 3 mM, 6 mM, or 12 mM glucose (prepared in stage 1). These droplets were then delivered to the glucose biosensor in series, exchanging the biosensor/wick after each measurement.

In the third single-mode application (III), a standard curve of H_2O_2 in PBS was prepared on-chip and analyzed electrochemically using screen-printed electrodes. A dilution series was generated from stock 10 mM H_2O_2 in PBS and PBS diluent. Briefly, diluent and a stock solution of 10 mM H_2O_2 in PBS were loaded into separate reservoirs on a device. Two double-unit droplets of 10 mM H_2O_2 in PBS were dispensed and stored on the array. A double-unit droplet of diluent was then dispensed and mixed with one of the 10 mM H_2O_2 double-unit droplets. The resulting quadruple-unit droplet of 5 mM H_2O_2 was then split into two double-unit droplets. A second double-unit droplet of diluent was dispensed and mixed with one of the 5 mM H_2O_2 double-unit droplets. The resulting quadruple-unit droplet of 2.5 mM H_2O_2 was then split into two double-unit droplets; one split-droplet was stored and the other was removed to waste. A third double-droplet of diluent was dispensed. The four double-unit droplets on the array (0 mM, 2.5 mM, 5 mM, and 10 mM) were then sequentially delivered to the screen-printed electrode in increasing concentration and measured. The wicks were replaced between each measurement.

PnP-DMF Dual-Mode Chemiluminescence and Electrochemistry Measurements. A DMF chemiluminescent enzyme-linked immunosorbent assay (ELISA) for insulin, combined with a PnP electrochemical measurement of glucose was developed using the following reagents. Dynabeads M-280 Tosylactivated magnetic beads (ThermoFisher, 2.8 μm diameter) were functionalized with mouse anti-insulin monoclonal IgG capture antibody (catalog no. 10-I30E, Fitzgerald) following the product insert. A total of 100 μg of capture antibody was used for 165 μL of magnetic bead suspension. The functionalized beads were stored in PBS containing 0.1% BSA (w/v) at 4 °C. Prior to use, the beads were washed three times with SuperBlock in TBS (Thermo-Fisher) with 0.1% 90R4 and suspended in the same solvent at a bead density of 1.03 mg/mL. Samples containing both glucose and insulin (Abbott Architect Controls, Abbott Diagnostics) were prepared in PBS with 4% (w/v) BSA and 0.1% 90R4 with (glucose in mM, insulin in μU/mL) concentrations of (0, 0), (1.5, 10), (4.5, 30), (7.5, 50), (11.25, 75), and (15, 100). For the immunoassays, a 100 μU/mL insulin in PBS with 4% (w/v) BSA and 0.1% 90R4 solution was used as positive control. A stock solution of mouse anti-insulin monoclonal IgG (catalog no. 10-I30F, Fitzgerald), used as detection antibody, was biotinylated (1 mg/mL ligand initial concentration) with a commercial kit (EZ-Link NHS-PEO$_4$-Biotinylation kit, ThermoFisher) by following the product insert. A working solution of detection antibody was prepared in SuperBlock in TBS with 0.1% 90R4 at a dilution of 1:10 000 from the stock for assays. A stock solution of streptavidin-horseradish peroxidase (HRP) (R&D Systems) was diluted 1:200 in PBS with 1% (w/v) BSA

and 0.1% 90R4. Chemiluminescent substrate luminol solution and stabilized H_2O_2 solution (SuperSignal ELISA Femto kit, ThermoFisher) were each supplemented with 0.05% 90R4. Wash buffer was PBS with 0.1% 90R4.

Dual-mode experiments with chemiluminescent ELISA in parallel with electrochemical measurements were implemented using devices generated with design 2 featuring a single glucose biosensor. These devices were controlled using a modified form of DropBot described previously[3] that includes a homemade motorized magnet positioned underneath the device for pelleting magnetic beads and an integrated photomultiplier tube (PMT) (H10721-110, Hamamatsu). Each assay required 17 steps, including the bead-based ELISA capture and detection of insulin and analysis of glucose from a single sample droplet. The detailed protocol, including all volumes and incubation times, is described in the Supporting Information.

RESULTS AND DISCUSSION

PnP-DMF-Electroanalysis: Design and Characterization. Microfluidic devices with integrated sensors have great promise for a wide range of applications[22] and are particularly well suited for the formation of small-form-factor systems that are appropriate for field-work. DMF devices have been reported that include embedded sensors[6−16] but they suffer from the limitation of compromised flexibility; once constructed, these devices can be used for only one purpose and no others. To solve this problem, we introduce a new strategy: plug-n-play digital microfluidics (PnP-DMF). The PnP-DMF approach, illustrated in Figure 1A (and shown in more detail in Supplementary Figure S1), relies on a custom DMF top plate that includes one or more cut-outs designed to fit the footprint of off-the-shelf electroanalytical sensors. As illustrated in Figure 1B, a paper wick is integrated into the system such that when a droplet is driven to the wick, analytes are rapidly transported to the sensor for analysis. In practice, unit and double-unit droplets (0.8−2.0 μL) on these devices were observed to completely absorb into the wick within 3 s of contact. We call the system "plug-n-play" because a given device can be easily and reversibly mated to any desired sensor within seconds. In fact, sensors can even be switched during a given experiment, a feature we call "hot swapping" (Figure 1C).

In the experiments described here, we explored the concept of PnP-DMF for four different types of sensors: two commercial biosensors marketed for home-diabetes care (bearing immobilized enzymes and cofactors designed to amplify and detect glucose or β-hydroxybutyrate), a custom paper-based biosensor (bearing enzymes and mediators suitable for detection of lactic acid), and a commercial screen-printed electrochemical cell (designed for general use). With this, we aim to illustrate how the PnP-DMF system opens up the possibility of having a sensor bank or toolkit, in which a large number of individual sensors (both commercial and custom-made) are called upon and integrated with DMF on an application-by-application basis. In addition to the flexibility of easily switching out sensors, a key advantage of this technique is cost; the sensors used here are inexpensive: $0.90, $2.60, $0.20, and $0.23 CAD (for the glucose biosensor, β-ketone biosensor, lactate biosensor, and the screen-printed sensor, respectively). We note that there are many similarly sized and priced sensors on the market, and the number and variety are expected to scale dramatically as interest in personalized testing skyrockets.[23,24] Thus, we propose that the technique
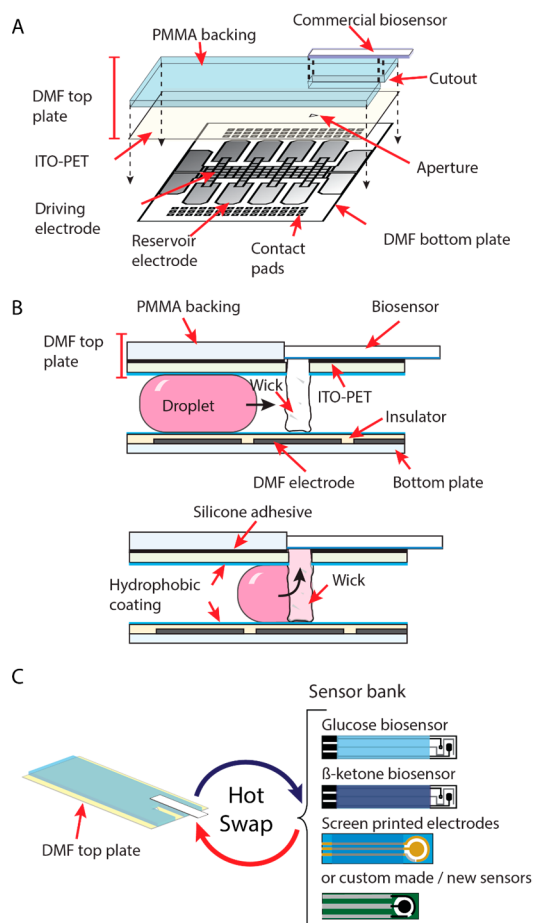
Figure 1. "Plug-n-play" digital microfluidics (PnP-DMF). (A) Cartoon (not to scale) illustrating how a PnP-DMF top plate is assembled and interfaced with a bottom plate. The sensor fits within a cutout in the PMMA backing layer. An ITO-PET film is used as a DMF ground electrode and a triangular aperture acts as a conduit between droplets on the DMF bottom plate and the electroanalytical cell. Contact pads interface the DMF driving and reservoir electrodes with the automation system. (B) Cartoon side view (not to scale) illustrating the composition of the DMF device and how droplets are wicked into the electroanalytical cell. (Top) The bottom plate comprises DMF electrodes coated with an insulator and hydrophobic coating. The DMF top plate comprises a PMMA backing affixed to an ITO-PET film. A wick fitted into the aperture acts as a conduit for the liquid droplet. The black arrow indicates direction of droplet movement. (Bottom) The droplet is moved to the DMF adjacent electrode and is wicked up (black arrow) into the electroanalytical cell. (C) Cartoon illustrating "hot swapping" sensors into the DMF top plate. A sensor bank provides options for a variety of applications that can be chosen on-the-fly.

described here represents a near-universal strategy for integrating sensors with DMF without compromising the flexibility inherent to the technique.

The two commercial biosensors used here contain three electrodes: one carbon electrode and two Ag/AgCl electrodes (Figure S2A). The electrodes are enclosed in a plastic chamber that (in conventional use) serves to measure 1.5 μL samples from a pin-prick of blood. Both glucose and β-hydroxybutyrate sensors rely on reactions of analyte with immobilized dehydrogenase enzymes coupled with NAD$^+$/NADH coenzyme and phenanthroline quinone electron mediators, which operate at a low potential (+0.200 V vs Ag/AgCl) and reduce

the risk of oxidizing other constituents in blood. These systems are designed for use with a dedicated potentiostat known as a glucometer, in a two-electrode cell measuring the potential between the carbon working electrode and the larger of the two Ag/AgCl electrodes. In conventional use, the third, smaller Ag/AgCl electrode is used as a "fill trigger" for metering.[25] In this work, we "hacked" the biosensors to make them operate in a three-electrode configuration using the "fill trigger" electrode as the reference electrode. In a three-electrode configuration, the reference electrode remains more stable as it is less likely to experience an Ohmic voltage-drop.

As a first step, calibration curves (prepared offline) were generated to characterize the two hacked commercial biosensors (Figure S2B,C). The glucose biosensor had a linear response (R^2 = 0.9974) across the range of concentrations measured (0.0−15.0 mM), with a LOD of 28 μM and LOQ of 72 μM. The β-ketone biosensor had a linear response (R^2 = 0.9873) over the clinically relevant range (0.0−2.0 mM), with a LOD of 4 μM and a LOQ of 152 μM. This performance is comparable to what has been reported for these sensors previously.[26] While the sensors were programmed and measurements collected using the open-source DStat potentiostat,[21] we note that a glucometer could also be used. This could be particularly advantageous for targeting an ultralow-cost platform, and there are examples in the literature of using these systems for a wide range of chemical analysis.[27−29]

Finally, the custom paper-based sensor (Figure S3) also had three electrodes and was prepared and used as described previously.[19] Note that in the future, simply changing the reagents and enzymes used to prepare the paper sensor may make it possible to detect other analytes. The screen-printed electrode cell had three electrodes (Figure S4) and was used as received. All of the sensors were controlled by the DStat potentiostat.[21]

Plug-n-Play DMF-Electroanalysis: Proof of Concept. With the new DMF-electroanalysis interface and four plug-n-play sensors in hand, we turned our attention to evaluating the suitability of this technique for integration with in-line digital microfluidic operations. As a first test, a mixture containing both glucose and β-hydroxybutyrate was evaluated serially and in parallel. In the serial measurement regime (Figure 2A), DMF was used to sequentially dispense two droplets of the sample and deliver them to the sensing region. In this experiment, the interface contained only a single cut-out such that the biosensors were exchanged during the experiment, demonstrating the "hot swapping" approach. The idea of a "removable" sensor that can be integrated with microchannels has been reported previously,[30−32] but this is the first example we are aware of a "hot-swapped" sensor (i.e., the use and exchange of two different sensors during the course of a single experiment) for any type of microfluidic device. In the parallel measurement regime (Figure 2B), two droplets were delivered simultaneously to two biosensors incorporated into a top plate for parallel analysis. (Of course, "hot swapping" could also be used for multiple sensors, further increasing the breadth of sensing options.) In this case the signals were read serially, but this is a function of the apparatus used here; future experiments might use multiple potentiostats to mate parallel detection with parallel fluid handling. To continue this test, a series of test solutions containing mixtures of glucose, β-hydroxybutyrate, and lactic acid were prepared and were cycled through a device serially, with hot-swapping between each test. Figure 2C shows a representative result of sequential
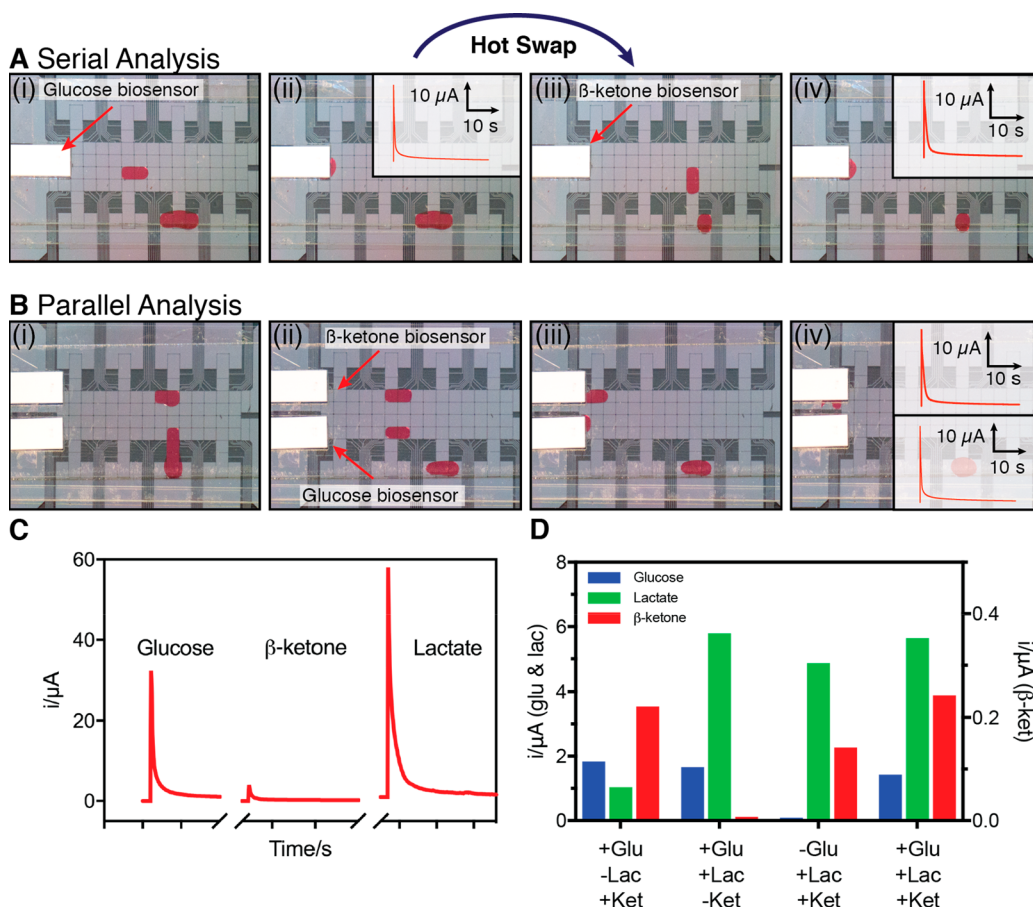
Figure 2. PnP-DMF-electroanalysis for serial and parallel measurements of mixtures of glucose ("Glu"), lactic acid ("Lac"), and β-hydroxybutyrate (also known as β-ketone, "Ket"). In labels, a "+" preceding the analyte indicates 5 mM for Glu or Ket or 12.5 mM for Lac; a "−" indicates 0 mM. (A) Photographs and corresponding amperograms (insets) collected during a serial measurement of +Glu/−Lac/+Ket, with hot-swapping between measurements. (i) A droplet is dispensed and moved to a glucose biosensor. (ii) The droplet is wicked into the biosensor and measured. (iii) The glucose biosensor is hot-swapped with a β-ketone biosensor and a second droplet is dispensed. (iv) The second droplet is wicked up into the biosensor and measured. (B) Photographs and corresponding amperograms (insets) collected during a parallel measurement of +Glu/−Lac/+Ket in a device bearing both Glu and Ket biosensors. (i) Two droplets are dispensed, (ii) moved to the sensors, (iii) wicked into the biosensors, and (iv) measured. Droplets contain red food dye for visualization. (C) Representative amperograms collected from serial analysis of +Glu/+Lac/+Ket, with hot-swapping between each measurement. The time scale on the x-axis is 5 s between ticks. (D) Current measured at 5 s for different permutations of the mixture (with signals for Glu and Lac plotted relative to the left axis and the signal for Ket plotted relative to the right axis). In all experiments, glucose and β-hydroxybutyrate amperograms were measured at +0.200 V (vs Ag/AgCl) while +0.450 V (vs C paste pseudo-RE) was used for lactate measurements.

amperometric readings performed using a +Glu/+Lac/+Ket solution, and Figure 2D shows the current readings at 5 s for the various permutations of analyte mixtures. These results highlight the flexibility of PnP-DMF, allowing for many different sensors to be interchanged while operating a single DMF device. Finally, because both sensor and absorbent wicks were always replaced between experiments, no cross-contamination was observed. This observation is not surprising for these kinds of small-molecule analytes; for other applications designed to test analytes prone to biofouling, surfactant additives[33,34] and/or specially designed device surfaces[35] may be useful for avoiding cross-contamination.

As illustrated above, PnP-DMF offers the ability to combine automated sample preparation and fluid handling with electroanalysis. As a proof-of-concept test for using PnP-DMF in complex procedures, we applied the technique to measure the concentration of glucose in a sample of blood by the method of standard additions. From a stock solution of a standard and diluent, a dilution series of droplets containing four concentrations of glucose was automatically generated on-chip (Figure 3A). This droplet-based dilution series was then mixed with aliquots of human blood (Figure 3B) and delivered to glucose biosensors for analysis (hot-swapping the sensors between each measurement). From the curve presented in Figure 3C, the native glucose concentration in the blood sample (accommodating the various dilutions) was calculated to be 2.75 mM (95% confidence interval: 2.38–3.18 mM). In total, 7.2 μL of blood was used to generate a standard curve (21.6 μL for triplicate measurements). Note that relatively large diluent-volume/sample-volume ratios (1:2) were used here (a function of constant driving electrode size); in the future, more conventional volume-ratios might be used on devices with variable driving electrode sizes (e.g., the device shown in Figure 5 of Yang et al.[36] supports the interface of droplets with a 1:12 volume ratio). Regardless, the proof-of-concept results presented here suggest that PnP-DMF may eventually be useful for quantifying analytes in precious samples by the method of standard additions.
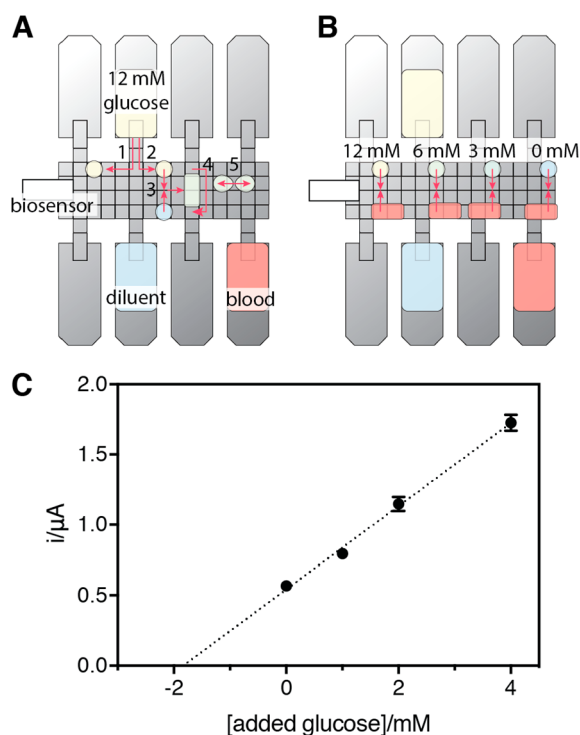
Figure 3. PnP-DMF electroanalysis for glucose measurements in blood with automated standard additions. (A) Cartoon illustrating the five-step procedure for glucose standard generation: (1) a single-unit droplet of 12 mM glucose solution is dispensed and stored, (2) a second single-unit droplet of 12 mM glucose is dispensed, (3) a single-unit droplet of diluent is dispensed and merged with a single-unit droplet of glucose, (4) the now double-unit droplet is mixed, and (5) the double-unit droplet is split into two single-unit droplets of 6 mM glucose. This general procedure is repeated to also generate a 3 mM glucose droplet. (B) Cartoon showing the addition of single-unit droplets of standards with double-unit droplets of blood sample. (C) PnP-DMF response using glucose biosensors to measure the glucose content of each droplet at +0.200 V vs Ag/AgCl, from which the initial glucose concentration can be calculated by the method of standard additions. Error bars represent ± 1 standard deviation ($n = 3$).

Figure 4. PnP-DMF-electroanalysis with off-the-shelf screen-printed electrodes for automated dilution and measurement of H_2O_2. Calibration curve generated from amperometric measurements (at +0.800 V vs Ag) of H_2O_2 solutions prepared on the DMF chip. Error bars represent ± 1 standard deviation ($n = 3$).

To further explore the generality of PnP-DMF, generic (unmodified) screen-printed electrodes were also integrated with the DMF top plate (Figure S4) to measure the concentration of H_2O_2. This analyte was selected because it is a common byproduct generated in a number of oxidase-catalyzed reactions,[37] and is therefore a candidate for measuring electron transfer in a wide range of different electrochemical biosensors in the future. A dilution series of H_2O_2 in PBS was formed on-chip and the resulting standard curve is shown in Figure 4. The PnP detector showed reasonable precision (2.5 mM, 21% CV; 5 mM, 17% CV; 10 mM, 12% CV, comparable to off-chip measurements) and can be used to measure H_2O_2 over a linear dynamic range of 0−5 mM ($R^2 = 0.9848$) with LOD and LOQ of 0.50 mM and 1.30 mM, respectively. The measurements described here were made relative to a Ag pseudoreference electrode; the precision could likely be increased in the future by using a Ag/AgCl reference, instead. Additionally, we predict that further optimization of sample delivery volume as a function of wicking pad dimensions and material should also improve the performance. Most importantly, the demonstrated compatibility with this generic electroanalytical cell suggests that future
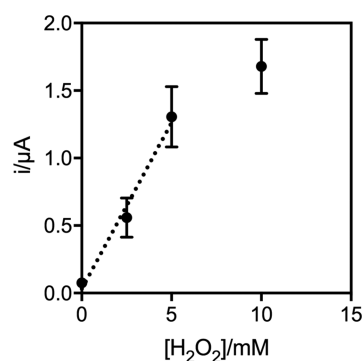
users will be able to co-opt this technique to generate custom, selective biosensors for any analyte of interest.

Multimodal Detection of Multiple Analytes. DMF is frequently used to implement complex, multistep optical immunoassays using paramagnetic beads.[3,18,38−43] Given the prominence of this type of assay in the literature, we decided to explore whether it can be run in tandem with PnP-DMF electrochemical sensing, effectively coupling two modes of detection in a single, integrated device. While there are many reports of multimodal detection in other kinds of microfluidic systems,[44−48] the method reported here represents the first such technique for digital microfluidics. We chose insulin and glucose as the two analytes for this test, given their importance in diagnosing and monitoring diabetes and related conditions.[49]

Figure 5A,B illustrates the PnP-DMF/multimodal, multiplexed assay. First, insulin is extracted from the droplet of sample by anti-insulin functionalized magnetic beads. A magnet underneath the DMF device is engaged to pellet the beads while the supernatant is removed. The supernatant is then assayed for glucose using the PnP-DMF glucose biosensor. Meanwhile, the magnetic beads are washed and then processed by a chemiluminescent immunoassay for insulin, with multiple wash steps in between each of the following stages: (1) biotinylated anti-insulin detection antibody labels the captured insulin; (2) horseradish peroxidase (HRP) conjugated to streptavidin labels the detection antibody; and (3) chemiluminescent substrate (H_2O_2 and luminol) is converted to chemiluminescent product and measured using an integrated PMT positioned above the DMF device. In all, the full procedure is implemented in 17 steps, which are described in detail in the Supporting Information. Calibration curves were generated for both electrochemical detection of glucose from the supernatant (Figure 5C) and the chemiluminescent immunoassay for insulin (Figure 5D). Both assays were predictable ($R^2_{glucose} = 0.9774$; $R^2_{insulin} = 0.9713$), with detection limits ($LOD_{glucose} = 0.15$ mM, $LOQ_{glucose} = 0.65$ mM; $LOD_{insulin} = 1.50$ μU/mL, $LOQ_{insulin} = 1.63$ μU/mL) much lower than would be required to assist in diagnosing diabetes and related conditions. Relative standard deviations were between 2 and 25% and 9−25% for glucose and insulin assays, respectively.

To our knowledge, the method described in Figure 5 represents the first report of a microfluidic technique
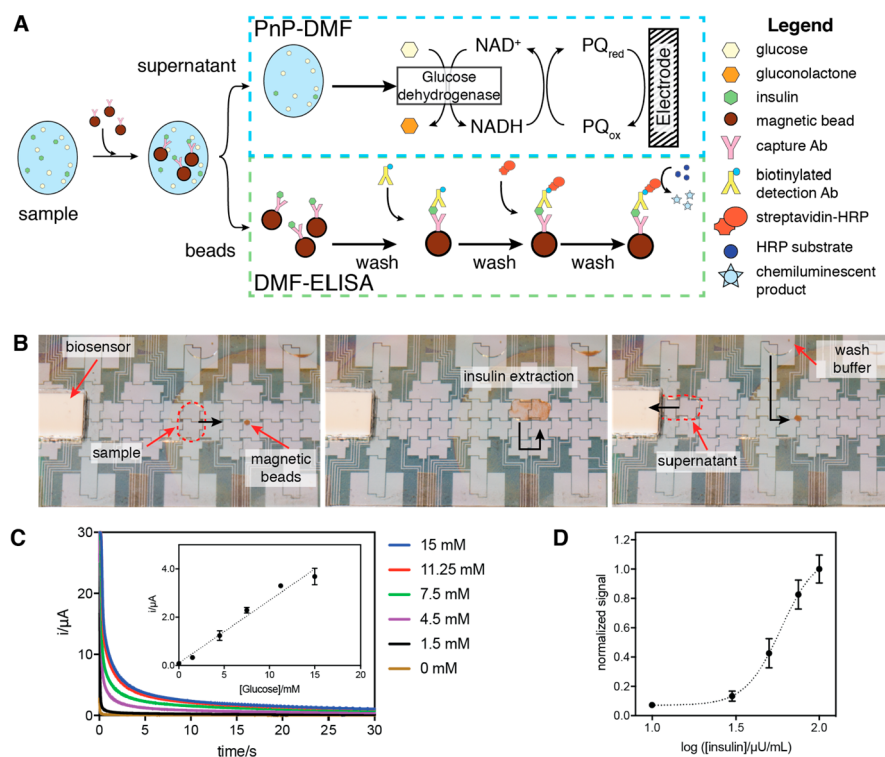
Figure 5. Multimodal and multianalyte sensing with PnP-DMF. (A) Cartoon outlining the dual sensing scheme for dual analyte detection from a single droplet. A droplet of sample containing both glucose and insulin is incubated with magnetic beads functionalized with anti-insulin capture antibodies. After insulin extraction, the supernatant is removed for PnP-DMF analysis (top) while the magnetic beads are processed by DMF-ELISA (bottom). For PnP-DMF analysis of glucose, the supernatant is delivered to the glucose biosensor where glucose dehydrogenase oxidizes glucose to gluconolactone, simultaneously reducing NAD$^+$ to NADH. Electron transfer to the electrode is achieved by the reduction of phenanthroline quinone from the oxidized (PQ_{ox}) to the reduced (PQ_{red}) state. Polarizing the electrode to +0.200 V vs Ag/AgCl oxidizes PQ_{red}. For DMF-ELISA, the beads with captured insulin are washed and then incubated with a biotinylated detection antibody. The beads are washed again before incubating with streptavidin conjugated to horseradish peroxidase. After further washing, the beads are incubated with chemiluminescent substrate (H_2O_2 and luminol) and the chemiluminescence is measured using a photomultiplier tube. (B) Photographs showing the principle of multimode, multianalyte analysis of a single droplet. Black arrows indicate droplet movement. Left panel: A double-unit droplet of sample is dispensed on a DMF device with an integrated glucose biosensor and is delivered to magnetic beads pelleted on the device. Middle panel: insulin is extracted from the droplet by repeatedly mixing the droplet. Right panel: the magnetic beads are pelleted with a magnet and the supernatant is removed to the biosensor; simultaneously, a droplet of wash buffer is dispensed and delivered to the magnetic beads. (C) Amperograms for samples measured at +0.200 V vs Ag/AgCl (blue, 15 mM; red, 11.25 mM; green, 7.5 mM; purple, 4.5 mM; black, 1.5 mM; tan, 0 mM glucose). Inset: Standard curve (dashed line) generated from average currents (black circles) recorded at 5 s. (D) Standard curve (dashed line) for insulin measured by chemiluminescent DMF-ELISA generated from average normalized PMT signals (black circles). In parts C and D, error bars represent ± 1 standard deviation ($n = 3$) for all concentrations.

(implemented in any format) in which different analytes are measured in the supernatant vs the precipitate (in this case, an immunoprecipitate captured on magnetic beads) collected from the same sample-aliquot. We wondered if this dual-use (supernatant and precipitate) system might have an effect on the glucose measurements relative to comparable measurements without a magnetic bead pull-down (e.g., Figures 2 and 3). To test this effect, we measured mean signals for glucose detection and droplet volumes across both techniques (i.e., with and without a magnetic bead pull-down) (Table S1). A *t*-test (two-tailed, unequal variance) revealed no significant difference ($p = 0.3539$, $n = 3$) between the glucose concentrations determined using the different regimes. On the other hand, a significant difference ($p = 0.0279$, $n = 3$) was observed between the mean volume of droplets dispensed from a reservoir and delivered directly to a biosensor compared to the mean volume of droplets that are removed as supernatant after incubation with the magnetic beads (Table S2). While this does not impact the glucose measurement, we suspect that this difference in volume is an effect of the volume of the

magnetic beads that are removed from the droplet plus some residual liquid trapped by the pelleted beads. This suggests that it may be possible to also perform multiple and sequential rounds of extraction for different analytes, to a degree, prior to analysis of the supernatant with a biosensor.

■ CONCLUSION

We have demonstrated a "plug-n-play" (PnP) method for integrating off-the-shelf and custom sensors with DMF. This greatly decreases the cost of integrating electrochemical sensing with DMF while maintaining the flexibility afforded by DMF. The PnP-DMF approach allows different types of electrodes to be interchanged (including on the fly in a "hot swapping mode") for multianalyte analysis. Additionally, PnP-DMF enables multimodal and multianalyte sensing from a single sample-droplet, suggesting broad applicability to applications requiring diverse formats and modalities. The results presented here add to the generic and programmable liquid handling capabilities of DMF, embodying the concept of the "lab on a chip."

■ ASSOCIATED CONTENT

Ⓢ Supporting Information

The Supporting Information is available free of charge on the ACS Publications website at DOI: 10.1021/acs.anal-chem.8b05375.

> Supporting information includes a schematic illustrating how the custom PnP-DMF top plates are manufactured (Figure S1); a schematic and off-chip characterization of the two commercial biosensors (Figure S2); schematics depicting how the paper-based biosensor (Figure S3) and the screen-printed electrode cells (Figure S4) are integrated with a DMF device; a detailed description for the dual-mode detection of insulin and glucose; and characterizations of the effects of multimodal analysis on glucose content (Table S1) and volume (Table S2) (PDF)

■ AUTHOR INFORMATION

Corresponding Author

*E-mail: aaron.wheeler@utoronto.ca. Phone: (416) 946 3864. Fax: (416) 946 3865.

ORCID ⊙

Aaron R. Wheeler: 0000-0001-5230-7475

Author Contributions

[⊥]R.P.S.d.C. and D.G.R. contributed equally to this work. D.G.R. conceived of the PnP-DMF interface. C.Z. and X.L. conceived of and manufactured the paper-based sensors. D.G.R. and R.P.S.d.C. performed all of the experimental work and data analysis. R.S. and R.P.S.d.C. acquired droplet images, and R.S. analyzed image data. D.G.R. and R.P.S.d.C. prepared the figures. D.G.R., R.P.S.d.C., and A.R.W. wrote the manuscript, with input from all authors.

Notes

The authors declare no competing financial interest.

■ ACKNOWLEDGMENTS

■ REFERENCES

(1) Gervais, L.; de Rooij, N.; Delamarche, E. *Adv. Mater.* **2011**, *23* (24), H151−H176.

(2) Kumar, A. A.; Hennek, J. W.; Smith, B. S.; Kumar, S.; Beattie, P.; Jain, S.; Rolland, J. P.; Stossel, T. P.; Chunda-Liyoka, C.; Whitesides, G. M. *Angew. Chem., Int. Ed.* **2015**, *54* (20), 5836−5853.

(3) Ng, A. H. C.; Fobel, R.; Fobel, C.; Lamanna, J.; Rackus, D. G.; Summers, A.; Dixon, C.; Dryden, M. D. M.; Lam, C.; Ho, M.; Mufti, N. S.; Lee, V.; Asri, M. A. M.; Sykes, E. A.; Chamberlain, M. D.; Joseph, R.; Ope, M.; Scobie, H. M.; Knipes, A.; Rota, P. A.; Marano, N.; Chege, P. M.; Njuguna, M.; Nzunza, R.; Kisangau, N.; Kiogora, J.; Karuingi, M.; Burton, J. W.; Borus, P.; Lam, E.; Wheeler, A. R. *Sci. Transl. Med.* **2018**, *10* (438), eaar6076.

(4) Fair, R. B. *Microfluid. Nanofluid.* **2007**, *3* (3), 245−281.

(5) Cho, S. K.; Moon, H.; Kim, C. J. *J. Microelectromech. Syst.* **2003**, *12* (1), 70−80.

(6) Dryden, M. D.; Rackus, D. D.; Shamsi, M. H.; Wheeler, A. R. *Anal. Chem.* **2013**, *85* (18), 8809−8816.

(7) Yu, Y. H.; Chen, J. F.; Li, J.; Yang, S.; Fan, S. K.; Zhou, J. J. *Micromech. Microeng.* **2013**, *23* (9), 095025.

(8) Shamsi, M. H.; Choi, K.; Ng, A. H.; Wheeler, A. R. *Lab Chip* **2014**, *14* (3), 547−554.

(9) Yu, Y.; Shamsi, M. H.; Krastev, D. L.; Dryden, M. D. M.; Leung, Y.; Wheeler, A. R. *Lab Chip* **2016**, *16* (3), 543−552.

(10) Yu, Y. H.; Chen, J. F.; Zhou, J. *J. Micromech. Microeng.* **2014**, *24* (1), 015020.

(11) Malic, L.; Veres, T.; Tabrizian, M. *Biosens. Bioelectron.* **2009**, *24* (7), 2218−2224.

(12) Shamsi, M. H.; Choi, K.; Ng, A. H.; Chamberlain, M. D.; Wheeler, A. R. *Biosens. Bioelectron.* **2016**, *77*, 845−852.

(13) Wondimu, S. F.; von der Ecken, S.; Ahrens, R.; Freude, W.; Guber, A. E.; Koos, C. *Lab Chip* **2017**, *17* (10), 1740−1748.

(14) Zhang, M.; Cui, W.; Chen, X.; Wang, C.; Pang, W.; Duan, X.; Zhang, D.; Zhang, H. *J. Micromech. Microeng.* **2015**, *25* (2), 025002.

(15) Choi, K.; Kim, J.-Y.; Ahn, J.-H.; Choi, J.-M.; Im, M.; Choi, Y.-K. *Lab Chip* **2012**, *12* (8), 1533−1539.

(16) Ceyssens, F.; Witters, D.; Van Grimbergen, T.; Knez, K.; Lammertyn, J.; Puers, R. *Sens. Actuators, B* **2013**, *181*, 166−171.

(17) Chin, C. D.; Linder, V.; Sia, S. K. *Lab Chip* **2012**, *12* (12), 2118−2134.

(18) Choi, K.; Ng, A. H. C.; Fobel, R.; Chang-Yen, D. A.; Yarnell, L. E.; Pearson, E. L.; Oleksak, C. M.; Fischer, A. T.; Luoma, R. P.; Robinson, J. M.; Audet, J.; Wheeler, A. R. *Anal. Chem.* **2013**, *85* (20), 9638−9646.

(19) Zhao, C.; Thuo, M. M.; Liu, X. *Sci. Technol. Adv. Mater.* **2013**, *14* (5), 054402.

(20) Fobel, R.; Fobel, C.; Wheeler, A. R. *Appl. Phys. Lett.* **2013**, *102* (19), 193513.

(21) Dryden, M. D. M.; Wheeler, A. R. *PLoS One* **2015**, *10* (10), No. e0140349.

(22) Rackus, D. G.; Shamsi, M. H.; Wheeler, A. R. *Chem. Soc. Rev.* **2015**, *44* (15), 5320−5340.

(23) Taylor, N. D.; Garruss, A. S.; Moretti, R.; Chan, S.; Arbing, M. A.; Cascio, D.; Rogers, J. K.; Isaacs, F. J.; Kosuri, S.; Baker, D.; Fields, S.; Church, G. M.; Raman, S. *Nat. Methods* **2016**, *13* (2), 177−183.

(24) Ahmed, M. U.; Saeem, I.; Wu, P. C.; Brown, A. S. *Crit. Rev. Biotechnol.* **2014**, *34* (2), 180−196.

(25) *Abbott Diabetes Care Evaluation of the FreeStyle Precision Neo Blood Glucose Monitoring System.* https://www.myfreestyle.com/neo/whitepaper/EVALUATION-OF-THE-FS-PRECISION-NEO-BLOOD-GLUCOSE-MONITORING-SYSTEM-HCP-CONSUMER.pdf.

(26) Forrow, N. J.; Sanghera, G. S.; Walters, S. J.; Watkin, J. L. *Biosens. Bioelectron.* **2005**, *20* (8), 1617−1625.

(27) Nie, Z.; Deiss, F.; Liu, X.; Akbulut, O.; Whitesides, G. M. *Lab Chip* **2010**, *10* (22), 3163−3169.

(28) Xiang, Y.; Lu, Y. *Nat. Chem.* **2011**, *3*, 697.

(29) Xiang, Y.; Lu, Y. *Anal. Chem.* **2012**, *84* (9), 4174−4178.

(30) Gowers, S. A. N.; Curto, V. F.; Seneci, C. A.; Wang, C.; Anastasova, S.; Vadgama, P.; Yang, G.-Z.; Boutelle, M. G. *Anal. Chem.* **2015**, *87* (15), 7763−7770.

(31) Erkal, J. L.; Selimovic, A.; Gross, B. C.; Lockwood, S. Y.; Walton, E. L.; McNamara, S.; Martin, R. S.; Spence, D. M. *Lab Chip* **2014**, *14* (12), 2023−2032.

(32) Kurbanoglu, S.; Mayorga-Martinez, C. C.; Medina-Sánchez, M.; Rivas, L.; Ozkan, S. A.; Merkoçi, A. *Biosens. Bioelectron.* **2015**, *67*, 670−676.

(33) Luk, V. N.; Mo, G. C. H.; Wheeler, A. R. *Langmuir* **2008**, *24* (12), 6382−6389.

(34) Au, S. H.; Kumar, P.; Wheeler, A. R. *Langmuir* **2011**, *27* (13), 8586−8594.

(35) Sarvothaman, M. K.; Kim, K. S.; Seale, B.; Brodersen, P. M.; Walker, G. C.; Wheeler, A. R. *Adv. Funct. Mater.* **2015**, *25* (4), 497−497.

(36) Yang, H.; Mudrik, J. M.; Jebrail, M. J.; Wheeler, A. R. *Anal. Chem.* **2011**, *83* (10), 3824−3830.

(37) Chen, W.; Cai, S.; Ren, Q.-Q.; Wen, W.; Zhao, Y.-D. *Analyst* **2012**, *137* (1), 49−58.

(38) Ng, A. H.; Choi, K.; Luoma, R. P.; Robinson, J. M.; Wheeler, A. R. *Anal. Chem.* **2012**, *84* (20), 8805−8812.

(39) Rackus, D. G.; de Campos, R. P. S.; Chan, C.; Karcz, M. M.; Seale, B.; Narahari, T.; Dixon, C.; Chamberlain, M. D.; Wheeler, A. R. *Lab Chip* **2017**, *17* (13), 2272−2280.

(40) Sista, R. S.; Eckhardt, A. E.; Srinivasan, V.; Pollack, M. G.; Palanki, S.; Pamula, V. K. *Lab Chip* **2008**, *8* (12), 2188−2196.

(41) Vergauwe, N.; Witters, D.; Ceyssens, F.; Vermeir, S.; Verbruggen, B.; Puers, R.; Lammertyn, J. *J. Micromech. Microeng.* **2011**, *21* (5), 054026.

(42) Fobel, R.; Kirby, A. E.; Ng, A. H. C.; Farnood, R. R.; Wheeler, A. R. *Adv. Mater.* **2014**, *26* (18), 2838−2843.

(43) Dixon, C.; Ng, A. H. C.; Fobel, R.; Miltenburg, M. B.; Wheeler, A. R. *Lab Chip* **2016**, *16* (23), 4560−4568.

(44) Lapos, J. A.; Manica, D. P.; Ewing, A. G. *Anal. Chem.* **2002**, *74* (14), 3348−3353.

(45) Pereira-Rodrigues, N.; Zurgil, N.; Chang, S.-C.; Henderson, J. R.; Bedioui, F.; McNeil, C. J.; Deutsch, M. *Anal. Chem.* **2005**, *77* (9), 2733−2738.

(46) Ordeig, O.; Ortiz, P.; Muñoz-Berbel, X.; Demming, S.; Büttgenbach, S.; Fernández-Sánchez, C.; Llobera, A. *Anal. Chem.* **2012**, *84* (8), 3546−3553.

(47) Liu, C.; Mo, Y.-y.; Chen, Z.-g.; Li, X.; Li, O.-l.; Zhou, X. *Anal. Chim. Acta* **2008**, *621* (2), 171−177.

(48) Apilux, A.; Dungchai, W.; Siangproh, W.; Praphairaksit, N.; Henry, C. S.; Chailapakul, O. *Anal. Chem.* **2010**, *82* (5), 1727−1732.

(49) MacDonald, P. E.; Joseph, J. W.; Rorsman, P. *Philos. Trans. R. Soc., B* **2005**, *360* (1464), 2211−25.